available at www.sciencedirect.com

ScienceDirect

journal homepage: www.elsevier.com/locate/biochempharm

Effect of 15-lipoxygenase metabolites, 15-(S)-HPETE and 15-(S)-HETE on chronic myelogenous leukemia cell line K-562: Reactive oxygen species (ROS) mediate caspase-dependent apoptosis

Suraneni V.K. Mahipal [a], *Jagu Subhashini* [b], *Madhava C. Reddy* [a], *Metukuri M. Reddy* [a], *Kotha Anilkumar* [a], *Karnati R. Roy* [a], *Gorla V. Reddy* [a], *Pallu Reddanna* [a,*]

[a] *Department of Animal Sciences, School of Life Sciences, University of Hyderabad, Hyderabad 500046, India*
[b] *Department of Pathology, Johns Hopkins School of Medicine, CRBII 308, Baltimore, MD 21231, USA*

ARTICLE INFO

Article history:
Received 25 January 2007
Accepted 4 April 2007

Keywords:
Apoptosis
15-(S)-HPETE
15-(S)-HETE
15-Lipoxygenase
ROS

ABSTRACT

Growth inhibitory effects of 15-lipoxygenase-1 [13-(S)-HPODE and 13-(S)-HODE] and 15-lipoxygenase-2 [15-(S)-HPETE and 15-(S)-HETE] (15-LOX-1 and LOX-2) metabolites and the underlying mechanisms were studied on chronic myeloid leukemia cell line (K-562). The hydroperoxy metabolites, 15-(S)-HPETE and 13-(S)-HPODE rapidly inhibited the growth of K-562 cells by 3 h with IC_{50} values, 10 and 15 μM, respectively. In contrast, the hydroxy metabolite of 15-LOX-2, 15-(S)-HETE, showed 50% inhibition only at 40 μM by 6 h and 13-(S)-HODE, hydroxy metabolite of 15-LOX-1, showed no significant effect up to 160 μM. The cells exposed to 10 μM of 15-(S)-HPETE and 40 μM of 15-(S)-HETE showed typical apoptotic features like release of cytochrome c, caspase-3 activation and PARP-1 (poly(ADP) ribose polymerase-1) cleavage. A flow cytometry based DCFH-DA analysis and inhibitory studies with DPI, a pharmacological inhibitor of NADPH oxidase, NAC (N-acetyl cysteine) and GSH revealed that NADPH oxidase-mediated generation of ROS is responsible for caspase-3 activation and subsequent induction of apoptosis in the K-562 cell line.

1. Introduction

Lipoxygenases (LOXs) are a group of closely related non-heme iron containing dioxygenases, which catalyze the addition of molecular oxygen into polyunsaturated fatty acids (PUFAs) containing *cis*, *cis* 1-4 pentadiene structures to yield their hydroperoxy derivatives. LOXs are classified depending on their site of oxygen insertion on arachidonic acid (AA) into 5-, 8-, 12- and 15-LOXs [1] and according to the positional specificity of arachidonate oxygenation into *S* and *R* isoforms [2]. 15-LOX has two isoforms, 15-LOX-1 and 15-LOX-2. Linoleate (LA) is the preferred substrate for 15-LOX which is metabolized to 13-(S)-HPODE that eventually gets reduced to 13-(S)-HODE. 15-LOX-2, on the other hand, oxygenates mainly AA to 15-(S)-HPETE that is reduced to 15-(S)-HETE (hereafter, 13-(S)-HPODE and 13-(S)-HODE are mentioned as 15-LOX-1

* *Corresponding author*. Tel.: +91 40 23010745; fax: +91 40 23010745.
E-mail address: prsl@uohyd.ernet.in (P. Reddanna).

Abbreviations: AA, arachidonic acid; DAPI, 4′,6-diamidino-2-phenylindole; DCFH-DA, 2′,7′-dichlorodihydrofluorescein diacetate; DPI, diphenylene iodonium; GSH, reduced glutathione; 13-(S)-HODE, 13-(S)-hydroxyoctadecadienoic acid; 13-(S)-HPODE, 13-(S)-hydroperoxyoctadecadienoic acid; 15-(S)-HETE, 15-(S)-hydroxyeicosatetraenoic acid; 15-(S)-HPETE, 15-(S)-hydroperoxyeicosatetraenoic acid; LA, linoleic acid; 15-LOX, 15-lipoxygenase; NAC, N-acetyl cysteine

0006-2952/$ – see front matter © 2007 Elsevier Inc. All rights reserved.
doi:10.1016/j.bcp.2007.04.005

metabolites and 15-(S)-HPETE and 15-(S)-HETE as 15-LOX-2 metabolites according to their substrate preferentiality to make a distinction, though these metabolites are not exclusively produced by the specified enzyme).

The role of various LOXs in regulating carcinogenesis was very well documented. 5-LOX, 8-LOX and 12-LOX were shown to have a procarcinogenic role, whereas 15-LOX was shown to be anti-carcinogenic [3]. Among the two isoforms, the role of 15-LOX-2 as anti-carcinogenic agent is established [4], the role of 15-LOX-1 in controlling carcinogenesis is still unclear. It was shown that 15-LOX-1 is expressed at higher levels in colorectal carcinoma and in tumors associated with prostate [5,6]. However, Shureiqi et al. reported the higher expression of 15-LOX-1 in normal tissues compared to the tumors [7]. Non-steroidal anti-inflammatory drugs (NSAIDs) and histone deacetylase (HDAC) inhibitors were shown to induce the expression of 15-LOX-1 in colorectal carcinomas and this up-regulation of 15-LOX-1 is critical for subsequent induction of apoptosis [8–10]. The expression of 15-LOX-2 and the production of its metabolite 15-(S)-HETE were found to be reduced in prostate carcinomas [11]. We have earlier shown that 15-LOX-2 metabolites [15-(S)-HPETE and 15-(S)-HETE] exert differential effects on BHK-21 cell proliferation. While 15-(S)-HPETE inhibited the proliferation of these cells potently, 15-(S)-HETE at the same concentration did not show any significant effect [12]. Recently, Maccarrone et al. demonstrated that, various LOX metabolites induce apoptosis in neuronal and leukemic cell types *in vitro* [13]. Although it is clear that 15-LOXs play a role in regulating carcinogenesis and induce apoptosis, the molecular mechanisms mediating these effects are still unknown. This study is designed to understand the molecular mechanisms mediating 15-LOX metabolite-induced apoptosis in human chronic myeloid leukemia cell line (K-562). Apoptosis induced by 15-LOX metabolites in K-562 cell line was found to be very rapid and hydroperoxy metabolites [15-(S)-HPETE and 13-(S)-HPODE] induce cell death more effectively compared to the corresponding hydroxy metabolites [15-(S)-HETE and 13-(S)-HODE]. The mechanistic aspects of 15-(S)-H(P)ETEs suggest that these metabolites activate the intrinsic cell death pathway through cytochrome *c* release and caspase-3 activation. These effects were found to be mediated by reactive oxygen species (ROS) generated through the activation of NADPH oxidase.

2. Materials and methods

2.1. Materials

Cell lines used in this study, K-562 (chronic myeloid leukemia), U-937 (human histiocytic leukemia), HL-60 (human promyelocytic leukemia) and Jurkat (human peripheral blood T cell leukemia) were obtained from the National Center for Cell Science, India. Phosphate buffered saline (PBS), RPMI medium and fetal bovine serum (FBS) were purchased from GIBCO Ltd. (BRL Life Technologies, Inc., USA). All the fine chemicals used in the study were procured from Sigma Chemical Co., USA. Nitrocellulose membranes and the ECL kit were from Amersham Biosciences, USA. Mouse monoclonal antibodies against cytochrome *c* were from Santa Cruz Biotechnology, Inc., USA. Polyclonal antibodies of poly(ADP) ribose polymerase (PARP) were from R&D systems, USA and polyclonal antibodies for caspase-3 were purchased from Cell Signaling Technology, Inc., USA. DCFH-DA was purchased from Molecular Probes, USA. Fluorogenic caspase-3 substrate—Ac-DEVD-AFC, caspase-3 inhibitor—Ac-DEVD-CHO and cell permeable caspase inhibitor—Z-VAD-FMK were from BD Biosciences, USA. Diphenylene iodonium (DPI) were procured from Calbiochem (EMD Biosciences, USA). The LOX metabolites used in this study were prepared through enzyme catalysis reactions by incubating arachidonic acid or linoleic acid with commercially procured Soybean LOX according to the procedures described elsewhere [14,15]. These metabolites were purified on straight phase HPLC (Shimadzu model equipped with SPD 6AV and CR4A chromatopac) using CLC-SIL (25 cm × 0.4 cm) column and they are confirmed by LC–MS analysis by Flow Injection Analysis in the negative ion mode employing electron spray ionization (ESI) on 1100 Series LC-MSD, Agilent Technologies.

2.2. Cell culture and treatment

The leukemic cell lines (K-562, U-937, HL-60 and Jurkat) were grown in suspension in RPMI 1640 medium supplemented with 10% heat inactivated fetal bovine serum (FBS), 100 IU/ml penicillin, 100 μg/ml streptomycin and 2 mM L-glutamine in a humidified atmosphere with 5% CO_2 at 37 °C. Exponentially growing K-562 cells resuspended in fresh culture medium with 1% FBS were treated with HPLC purified 15-LOX metabolites [15-(S)-HPETE, 15-(S)-HETE, 13-(S)-HPODE and 13-(S)-HODE] dissolved in ethanol. The final concentration of the vehicle never exceeded 0.1%. Wherever the inhibitors were used in this study, toxic-profiling in terms of dosage and time was carried out and the non-toxic and efficient doses were used for studies.

2.3. Cell viability and cytotoxicity

15-LOX metabolite-induced growth inhibitory effects were assessed using the MTT assay as described [16]. For the MTT assay, 5×10^3 exponentially growing cells were plated in 100 μl of the growth medium in the presence or absence of 1–20 μM of hydroperoxy 15-LOX metabolites [15-(S)-HPETE and 13-(S)-HPODE] and 10–160 μM of hydroxy 15-LOX metabolites [15-(S)-HETE and 13-(S)-HODE] in 96 well plates and cultured at 37 °C in 5% CO_2 for 3–24 h. The cells were then incubated with 20 μl of MTT (5 mg/ml) at 37 °C for 4 h. After dissolving the crystals in a triplex solution containing 12% SDS, 5% isobutanol and 12 mM HCl, the plates were read in a microtiter plate reader at 570 nm. Each concentration was tested in three independent experiments run in four replicates. Standard errors of means were calculated and reported as %growth versus control. The concentration of the compound that inhibited cell growth by 50% (IC_{50}) was determined from cell survival plots.

2.4. DNA fragmentation assay

K-562 cells were treated with either 15-(S)-HPETE (5 and 10 μM for 3 h) or 15-(S)-HETE (20 and 40 μM for 6 h) for indicated time periods and used for the isolation of the DNA. DNA laddering was detected by isolating fragmented DNA using the SDS/

proteinase K/RNase A extraction method, which allows the isolation of only fragmented DNA without contaminating genomic DNA [17]. Fragmented DNA was resolved on 1% agarose gel in TBE (44.6 mM Tris, 44.5 mM boric acid and 1 mM EDTA), stained with ethidium bromide (0.5 mg/ml) and visualized by UV light.

2.5. Quantification of apoptosis by flow cytometry

Flow cytometric analysis using propidium iodide was performed to quantitate apoptosis. Cells that were less intensely stained than G1 cells (sub G0/G1 cells) in flow cytometric histograms were considered apoptotic cells. The DNA staining was carried out as described previously [18] with minor modifications. After treatment, cells were prepared as a single cell suspension in 200 μl PBS, fixed with 2 ml of ice-cold 70% ethanol and incubated overnight at 4 °C. The cells were resuspended in 500 μl PBS supplemented with 0.1% Triton X-100 and RNase A (50 μg/ml), incubated at 37 °C for 30 min and stained with 50 μg/ml propidium iodide (PI) in the dark at 4 °C for 30 min. The red fluorescence of individual cells was measured with a FACS Calibur flow cytometer (Becton Dickinson, San Jose, USA). A minimum of 10,000 events were counted per sample.

2.6. Preparation of whole cell extracts and immunoblot analysis

The cell lysis was carried out based on a method described earlier [19]. Whole cell extracts were prepared in RIPA lysis buffer and protein estimation was done by Bradford method [20], cell lysates were resolved on 8–12% SDS-PAGE gels along with protein molecular weight standards and then transferred onto nitrocellulose membranes. The transfer was confirmed with Ponceau S staining, membranes were blocked and incubated with primary antibodies (for caspase-3 and PARP) followed by peroxidase conjugated secondary antibodies. Signals were detected using peroxidase substrate TMB/H_2O_2 or with ECL Western blotting detection kit (Amersham Biosciences, USA) according to the manufacturer's recommendations. The blots were probed with β-actin antibodies to confirm equal loading.

2.7. Detection of cytochrome c release using Western blot analysis

Upon exposure to 10 μM 15-(S)-HPETE or 40 μM 15-(S)-HETE, the cells were collected and washed once with PBS and subsequently with buffer A (0.25 M sucrose, 30 mM Tris–HCl, pH 7.9, 1 mM EDTA). Cells were then resuspended in buffer A containing 1 mM PMSF, 1 mg/ml leupeptin, 1 mg/ml pepstatin, 1 mg/ml aprotinin, homogenized with a glass dounce homogenizer and centrifuged at 21,000 × *g* for 10 min. Thirty micrograms of cytosolic protein extract was used for Western blot analysis as described above. Cytochrome *c* was detected using a mouse monoclonal antibody directed against human cytochrome *c*.

2.8. Measurement of reactive oxygen species (ROS)

ROS production upon treatment with 15-LOX metabolites was detected using the dye, DCFH-DA. DCFH-DA, a non-fluorescent cell-permeant compound, is cleaved by endogenous esterases inside the cell and the de-esterified product becomes the fluorescent compound 2′7′-dichlorofluorescein (DCF) upon oxidation by ROS [21,22]. Prior to the treatments, cells were incubated with 10 μM DCFH-DA at 37 °C for 15 min and then washed twice in PBS supplemented with 10 mM glucose. Washed cells were resuspended in the same buffer and treated with either 10 μM 15-(S)-HPETE or 40 μM 15-(S)-HETE for various time periods and ROS measurement was carried out on FACS Calibur flow cytometer. Data were collected using the data acquisition program CELLQuest (Becton Dickinson, San Jose, CA). DCF data were collected with the following excitation and emission wavelengths: λ_{exc} = 488 nm, λ_{em} = 525 nm. Ten thousands events were analyzed per sample.

2.9. Estimation of the cellular glutathiones (GSH and GSSG)

After the treatments with either 15-(S)-HPETE (10 μM) or 15-(S)-HETE (40 μM), equal number of cells were collected and washed twice with phosphate buffered saline, lysed and protein concentrations were estimated. The cell lysates were then incubated with sulfosalicylic acid (10%, w/v) for 10 min to precipitate the proteins and centrifuged at 10,000 × *g* for 5 min to remove denatured proteins. GSH and GSSG were estimated by the enzymatic method (DTNB recycling assay) [23] using a standard curve with known amounts of GSH.

2.10. Caspase-3 activity assay

After the stipulated treatments, 2×10^6 cells were lysed in 100 μl of CHAPS lysis buffer by three to four freeze–thaw cycles. The extracts were centrifuged at 12,000 × *g* and the resulting supernatants were used for the assay. The assay was performed according to the manufacturer's protocol (BD biosciences, USA). The assay buffer contained 20 mM PIPES, 100 mM NaCl, 10 mM DTT, 1 mM EDTA, 0.1% (w/v) CHAPS, 10% sucrose, pH-7.2. 50 μg of the protein and 10 μl of the substrate (Ac-DEVD-AFC, 1 mg/ml) were added to 1 ml of the assay buffer and incubated for 1 h at 37 °C. Measurements were done on spectrofluorimeter with an excitation wavelength of 400 nm and an emission wavelength of 480–520 nm.

2.11. Glutathione peroxidase (GPx) assay

5×10^6 cells were lysed in 200 μl of lysis buffer containing 10 mM Tris, pH 7.5, 150 mM NaCl, 0.1 mM EDTA, 0.5% Triton X-100, incubating on ice for 10 min. Cell lysates were spun at 12,000 × *g* for 10 min and the supernatants were used for the assay of GPx. GPx activity was measured by a procedure described by Paglia and Valentine [24] and the activity was calculated with an extinction coefficient of 6.22 mM^{-1} cm^{-1}. One unit of GPx activity was defined as 1 nmol of NADPH oxidized per minute.

2.12. Statistical analysis

Data were presented as the mean ± S.E. of three independent experiments. Statistical analysis of differences was carried out

by one-way analysis of variance (ANOVA). A p-value of less than 0.05 was considered to be significant.

3. Results

3.1. *Effect of 15-lipoxygenase metabolites on the growth of K-562 cell line*

Cells were cultured in RPMI 1640 + 10% FBS and treatments were carried out in medium containing 1% FBS with 1–20 μM 15-(S)-HPETE and 13-(S)-HPODE, 1–160 μM 15-(S)-HETE and 13-(S)-HODE for 3–24 h and the cytotoxicity and cell proliferation were evaluated by the MTT assay. Under these experimental conditions, 15-(S)-HPETE and 13-(S)-HPODE inhibited the growth of K-562 cells rapidly by 3 h with IC_{50} values 10 and 15 μM, respectively (Fig. 1A and C). While 15-(S)-HETE showed maximum cytotoxicity at higher concentrations than its corresponding hydroperoxide (15-(S)-HPETE) with an IC_{50} value of 40 μM by 6 h (Fig. 1B), 13-(S)-HODE did not show any significant effect until extremely high concentrations (160 μM) were employed (Fig. 1D). Further studies to elucidate the mechanism of 15-LOX metabolite-induced cell death were carried out with 15-LOX-2 metabolites, 15-(S)-HPETE and 15-(S)-HETE, with the above mentioned doses and time periods.

3.2. *Flow cytometric analysis of 15-LOX-2 metabolite-induced apoptosis*

Phase-contrast and Fluorescence microscopic (with DNA binding dye, DAPI) studies carried out with 15-LOX-2 metabolite (15-(S)-H(P)ETE) treated cells showed characteristic features of apoptosis, such as membrane blebbing, nuclear condensation, marginalization and fragmentation (data not

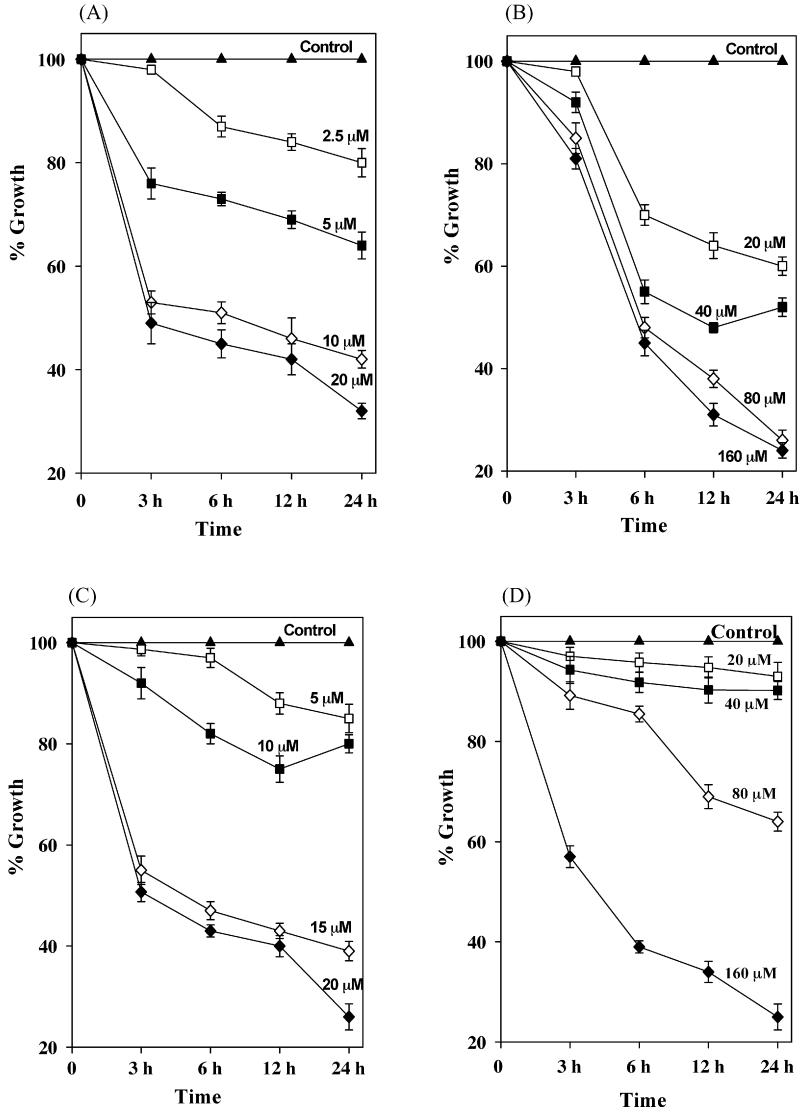

Fig. 1 – Effect of 15-LOX-1 (13-(S)-HPODE and 13-(S)-HODE) and 15-LOX-2 (15-(S)-HPETE and 15-(S)-HETE) metabolites on the growth of human chronic myeloid leukemia-K-562 cell line. Cells (5×10^3) were treated with various concentrations of 15-(S)-HPETE (A), 15-(S)-HETE (B), 13-(S)-HPODE (C) and 13-(S)-HODE (D) and the cell viability was measured by MTT assay at 3, 6, 12 and 24 h post treatment. The values represent the mean ± S.E. from three independent experiments.

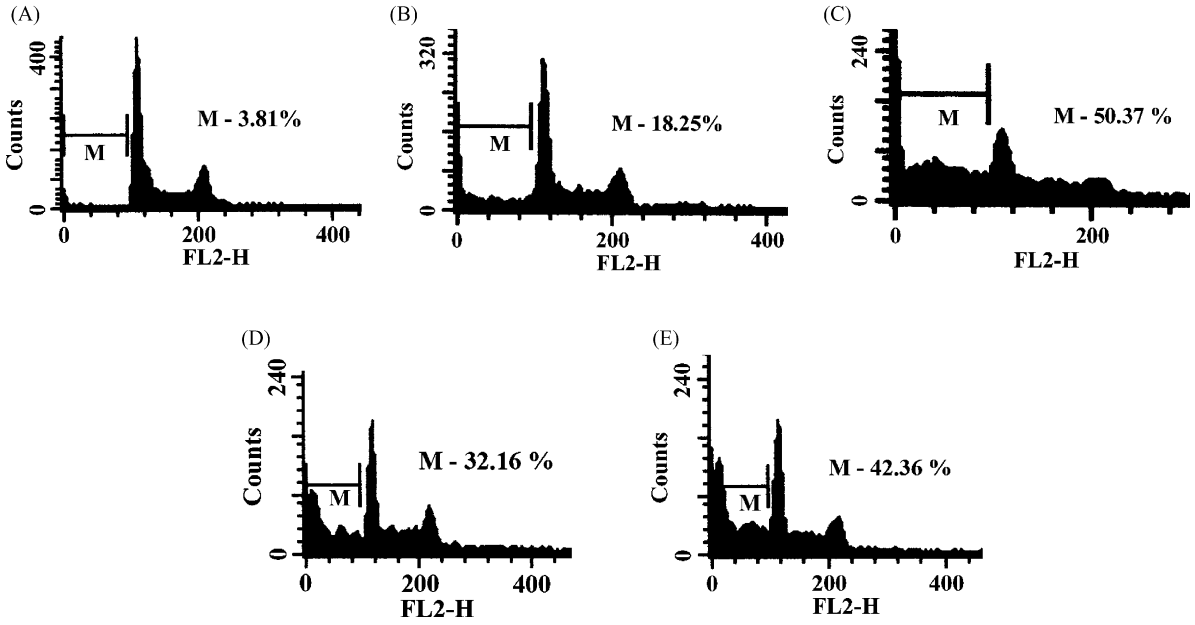

Fig. 2 – Flow cytometric analysis of 15-LOX-2 metabolite-induced apoptosis in K-562 cells by propidium iodide (PI) staining. The cells (1.3×10^6 cells) treated with 5, 10 μM 15-(*S*)-HPETE for 3 h and 20, 40 μM 15-(*S*)-HETE for 6 h were fixed in 1 ml of 70% ethanol with 0.5% Tween-20 at 4 °C for 30 min and suspended in PBS. The cells were then stained with PI solution for 1 h and analyzed for DNA content by flow cytometry. Data represent the result from one of three similar experiments. (A) Control; (B) 15-(*S*)-HPETE (5 μM); (C) 15-(*S*)-HPETE (10 μM); (D) 15-(*S*)-HETE (20 μM); (E) 15-(*S*)-HETE (40 μM).

included). The induction of apoptosis in 15-LOX-2 metabolite-treated K-562 cells was verified further and quantified by flow cytometric analysis of DNA content. Fig. 2 illustrates the DNA content of 15-LOX-2 metabolite-treated permeabilized cells obtained after PI staining. Typical sub-diploid apoptotic peaks were observed in K-562 cells treated with 15-(*S*)-HPETE (5 and 10 μM for 3 h) and 15-(*S*)-HETE (20 and 40 μM for 6 h). FACS analysis of control cells, on the other hand, showed prominent G1, followed by S and G2/M phases. Only around 4% of these cells showed hypodiploid DNA (sub G0/G1 peak) (Fig. 2A). This value of 4% hypodiploid DNA in control cells increased to 18.25 and 50.37% in 15-(*S*)-HPETE (5 and 10 μM) treated cells (Fig. 2B and C) and to 32.16 and 42.36% in 15-(*S*)-HETE (20 and 40 μM) treated cells (Fig. 2D and E). Increase of hypodiploid apoptotic cells in response to 15-LOX-2 metabolite treatment is concentration-dependent and a decrease in the percentage of cells is noticed in other phases of the cell cycle.

3.3. *Cytochrome c release, caspase-3 activation and PARP cleavage in response to 15-(S)-HPETE and 15-(S)-HETE treatment*

The levels of cytochrome *c* in the cytosol were elevated within 1 h of treatment with 10 μM 15-(*S*)-HPETE (Fig. 3A) (lanes 2 and 3) and the levels were further increased at later time points (lanes 4 and 5). In case of 15-(*S*)-HETE (40 μM) treatment, the same time dependent increase in the level of cytochrome *c* in the cytosol (lanes 2–4) in comparison to the control (lane 1) was observed by Western blot analysis (Fig. 3B). Western blot analysis showed time dependent activation of caspase-3 in cells treated with both 10 μM 15-(*S*)-HPETE (Fig. 3C) and 40 μM 15-(*S*)-HETE (Fig. 3D). Caspase-3 activity was quantified by a fluorimetric assay with the caspase-3 specific substrate Ac-DEVD-AFC. Treatment with 10 μM 15-(*S*)-HPETE resulted in nearly 5-fold (5 ± 0.34, $n = 3$, $p < 0.05$) (Fig. 3E) increase in caspase-3 activity compared to control by 2 h. Cells treated with 40 μM 15-(*S*)-HETE showed 3.5–4-fold (3.5 ± 0.4, $n = 3$, $p < 0.05$) increase in caspase-3 activity by 4 h (Fig. 3F). 15-LOX-2 metabolite-induced apoptosis was abrogated completely when cells were pretreated with 25 μM Z-VAD-FMK (a broad spectrum caspase inhibitor) for 1 h. As depicted in Fig. 3G, after treatment with 10 μM 15-(*S*)-HPETE and 40 μM 15-(*S*)-HETE, the percentage of apoptotic cells from 6.2 ± 1.2 in control raised to 43.5 ± 3.4 ($n = 3$, $p < 0.05$) and 37 ± 2.5 ($n = 3$, $p < 0.05$), respectively. However, pretreatment with 25 μM Z-VAD-FMK resulted in decrease of apoptosis to $7.5 \pm 1.3\%$ ($n = 3$, $p < 0.05$) from 43.5% in case of 10 μM 15-(*S*)-HPETE and to $5.93 \pm 1.2\%$ from 37% in case of 40 μM 15-(*S*)-HETE. These results clearly show that caspase-3 activation occurs and is an essential event in 15-LOX-2 metabolite-induced apoptosis. PARP is a 116 kDa protein and is cleaved by caspases during apoptosis to generate 89 and 23 kDa fragments. PARP cleavage was monitored with PARP antibodies, which recognize the 23 kDa fragment of the cleaved PARP and intact 116 kDa PARP protein. Fig. 3H and I illustrates the dose dependent increase in the accumulation of the 23 kDa cleavage product with 15-LOX-2 metabolite treatment. In contrast, the control cells showed very small amounts of 23 kDa fragment of PARP (lane 1).

3.4. *15-LOX-2 metabolites induced DNA fragmentation in K-562 cells*

Agarose gel electrophoresis of DNA extracted from K-562 cells treated with 15-(*S*)-HPETE (5 and 10 μM for 3 h) and 15-(*S*)-HETE

(20 and 40 μM for 6 h) showed a progressive increase in the non-random DNA fragmentation into a ladder of 180–200 bp Fig. 4, lanes 2–5). Such a pattern corresponds to internucleosomal cleavage, reflecting the endonuclease activity characteristic of apoptosis. Control cells did not show any internucleosomal DNA fragmentation (lane 1).

3.5. *Reactive oxygen species (ROS) are generated upon 15-LOX-2 metabolite treatment*

ROS induction upon 15-LOX-2 metabolite treatments was examined through DCFH-DA analysis. Upon treatment with 10 μM 15-(S)-HPETE, significant generation of ROS was observed within minutes as evidenced by the shift in DCF fluorescence, 6.29 ± 0.32 ($n = 3$, $p < 0.05$) folds over control in 30 min and 8.95 ± 0.57 folds over control in 60 min (Fig. 5A). Treatment with 15-(S)-HETE (40 μM) resulted in significant generation of ROS compared to control although the magnitude of ROS generation is somewhat less than that observed with 15-(S)-HPETE (Fig. 5B). This differential induction of ROS by the hydroperoxy [15-(S)-HPETE] and hydroxy [15-(S)-HETE] metabolites may play a key role in the difference in their growth inhibitory effects and induction of apoptosis. ROS production in case of 15-LOX-2 metabolite treatment is associated with changes in reduced glutathione (GSH) levels. This is evident by an increase in the levels of GSH in the earlier time points with a decrease at later time points. This decrease in the GSH levels was not associated with any significant change in the levels of oxidized glutathione (GSSG), which further resulted in decrease in GSH/GSSG ratio as depicted in Fig. 5C. To examine the role of ROS generation and glutathione depletion in 15-LOX-2 metabolite-induced apoptosis, the cells were pretreated with 50 μM NAC (a glutathione precursor and an anti-oxidant) for 3 h followed by 10 μM 15-(S)-HPETE or 40 μM 15-(S)-HETE treatments and analyzed for ROS production and inhibition of apoptosis. NAC pretreatment resulted in

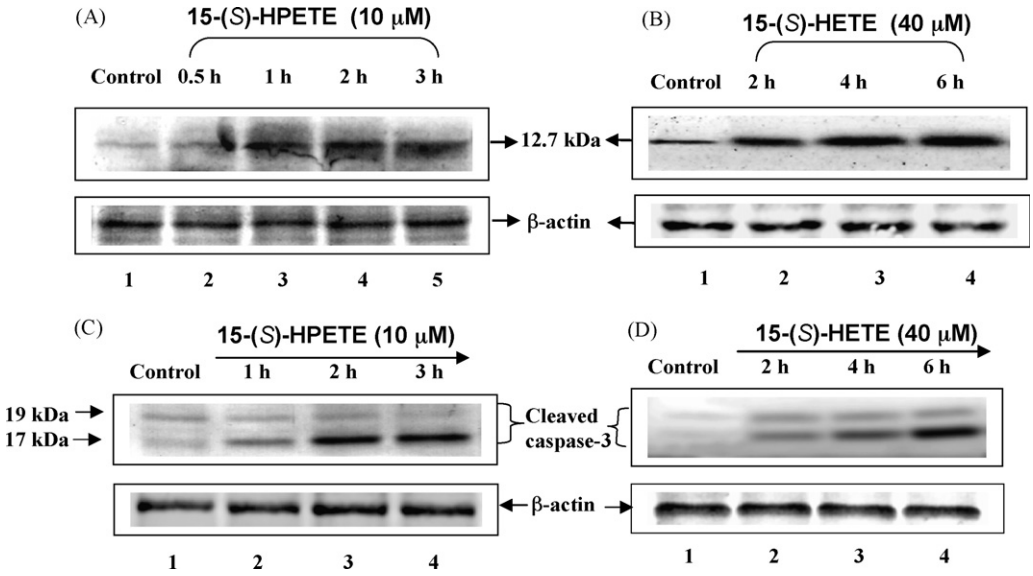

Fig. 3 – Effects of 15-(S)-HPETE (10 μM) and 15-(S)-HETE (40 μM) on cytochrome c release, caspase-3 cleavage and PARP cleavage. (A and B) Cytochrome c release. Equal amounts of protein (30 μg) from the K-562 cells treated with 10 μM 15-(S)-HPETE (A) and 40 μM 15-(S)-HETE (B) for the indicated times were analyzed on 15% SDS-PAGE and immunoblotted with anti-cytochrome c antibody. (C and D) Detection of caspase-3 cleavage by Western blotting. Treated cell extracts were resolved on 12% SDS-PAGE and probed with anti-caspase-3 antibodies that specifically detect cleaved caspase-3 fragments. (C) 15-(S)-HPETE (10 μM); (D) 15-(S)-HETE (40 μM). Actin was probed to confirm equal loding. (E and F) Detection of caspase-3 cleavage by spectroflourimetric assay. K-562 cells after treatement with either 10 μM 15-(S)-HPETE (for 1, 2 h) or 40 μM 15-(S)-HETE (for 2, 4 h) were lysed and assayed for caspase-3 activity with a fluorogenic caspase-3 substrate—Ac-DEVD-AFC. Ac-DEVD-CHO, a specific inhibitor for caspase-3 was used as an assay control. (E) 15-(S)-HPETE: 1, control; 2, 10 μM 15-(S)-HPETE—1 h; 3, 10 μM 15-(S)-HPETE—2 h; 4, 10 μM 15-(S)-HPETE—2 h + Ac-DEVD-CHO (1 μg/ml). (F) 15-(S)-HETE: 1, control; 2, 40 μM 15-(S)-HETE—2 h; 3, 40 μM 15-(S)-HETE—4 h; 4, 40 μM 15-(S)-HETE—4 h + Ac-DEVD-CHO (1 μg/ml). (G) Protective effect of Z-VAD-FMK, a broad spectrum caspase inhibitor on 15-LOX-2 metabolite-induced apoptosis. K-562 cells were preincubated with a cell permeable caspase inhibitor Z-VAD-FMK (25 μM) for 1 h and then treated with either 10 μM 15-(S)-HPETE for 3 h or with 40 μM 15-(S)-HETE for 6 h and scored for apoptotic cells on flow cytometer using propidium iodide staining. Data presented here represent the mean ± S.E. from three independent experiments and the significance was established at $^{*}p < 0.05$. (H and I) Detection of PARP cleavage in K-562 cells using Western blot analysis after treatment with 15-(S)-HPETE (10 μM) (H) and 15-(S)-HETE (40 μM) (I). Cells (3.5×10^6) were seeded in 60 mm dishes and treated for indicated times in a time dependent manner. Fifty micrograms of total protein extract were separated on a 12% SDS-polyacryamide gel was electroblotted onto a nitrocellulose membrane. PARP (116 kDa) and the cleavage product of PARP (23 kDa) were detected using a goat polyclonal anti-PARP antibody. Actin was used as a control for equal loading.

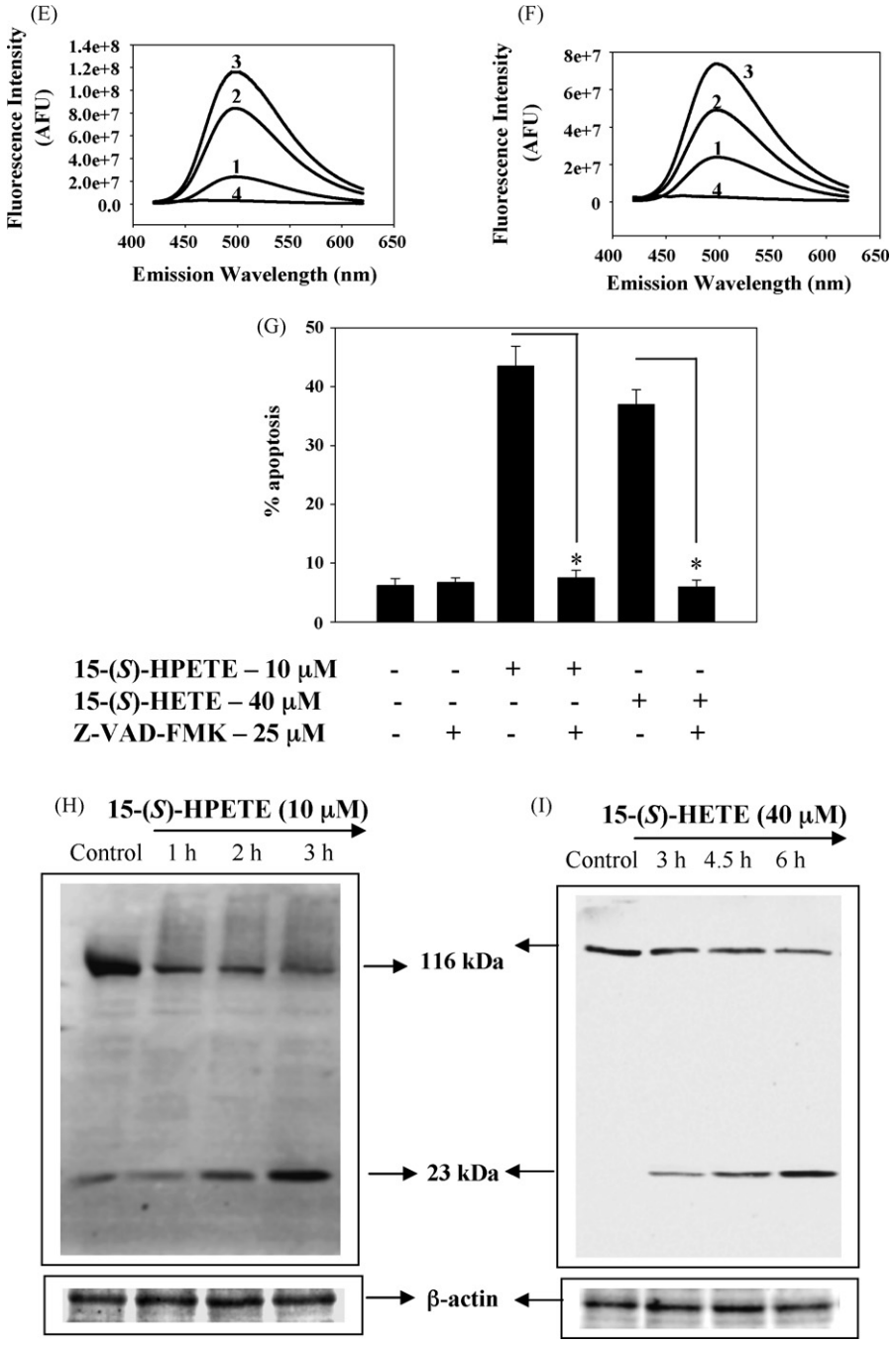

Fig. 3. (Continued).

reduction of cellular ROS levels by 52% in 15-(S)-HPETE (Fig. 6A) and by 63% in 15-(S)-HETE treatment (Fig. 6B) and reduced apoptotic induction by 63.2 and 47% in 15-(S)-HPETE (Fig. 7A) and 15-(S)-HETE treatments (Fig. 7B), respectively. Apoptosis induced by 10 μM 15-(S)-HPETE (Fig. 7A) and 40 μM 15-(S)-HETE (Fig. 7B) was reduced by 66.8 and 55%, respectively, when cells were pretreated with 200 μM GSH, corroborating with previous observations of induction of ROS and depletion of reduced glutathione during 15-LOX-2 metabolite-induced apoptosis. These anti-oxidants inhibit the activation of caspase-3 (Fig. 8A and B) and thereby abrogating the subsequent induction of apoptosis.

3.6. *NADPH oxidase activation by 15-LOX-2 metabolites initiates ROS generation and subsequent induction of apoptosis*

Pretreatment of K-562 cells with 10 μM DPI for 1 h followed by treatments with 10 μM 15-(S)-HPETE for 1 h or 40 μM 15-(S)-HETE for 1.5 h, resulted in the reduced intracellular ROS levels (Fig. 9A and B). Pretreatment of DPI inhibited 85% of ROS production induced by 15-(S)-HPETE and 76% of ROS production induced by 15-(S)-HETE. These results demonstrate that NADPH oxidase is the site of ROS production in case of both 15-(S)-HPETE and 15-(S)-HETE treatments. When K-562 cells were

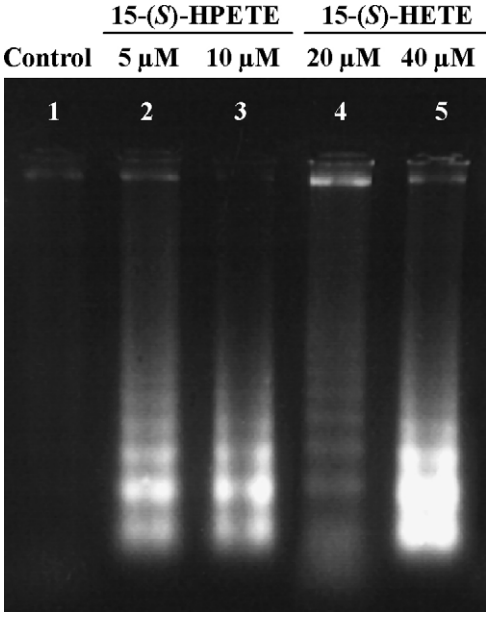

Fig. 4 – Induction of DNA fragmentation by 15-LOX-2 metabolites. DNA was isolated from K-562 cells treated with various concentrations of 15-(S)-HPETE (for 3 h) and 15-(S)-HETE (for 6 h) as indicated, and separated on 1.5% agarose gel. DNA was stained with ethidium bromide and visualized under UV light.

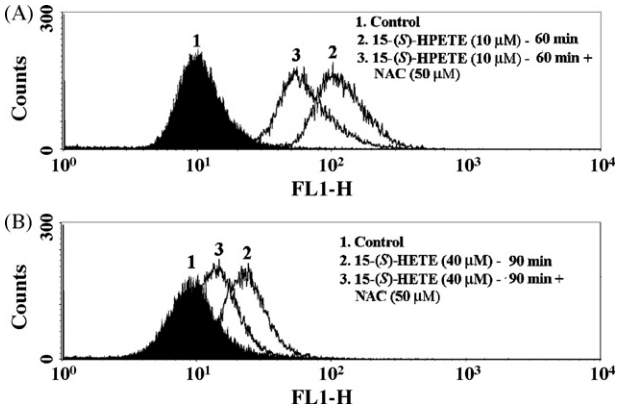

Fig. 6 – ROS analysis by DCFH-DA of K-562 cells pretreated with 50 μM N-acetyl cysteine (NAC—glutathione precursor) for 3 h followed by treatment with 15-LOX-2 metabolites. (A) 1, control; 2, 10 μM 15-(S)-HPETE—60 min; 3, 10 μM 15-(S)-HPETE—60 min + 50 μM NAC. (B) 1, control; 2, 40 μM 15-(S)-HETE—90 min; 3, 40 μM 15-(S)-HETE—90 min + 50 μM NAC.

pretreated with 10 μM DPI and analyzed by propidium iodide staining, a dose dependent decrease in the induction of apoptosis was observed (Fig. 7A and B). The abrogation of apoptosis by DPI pretreatment was preceded by concomitant inhibition of caspase-3 activation (Fig. 8A and B). As DPI was also shown to inhibit inducible nitric oxide synthase (iNOS) [25], we examined the effects of L-NMMA, a more specific inhibitor of iNOS on 15-LOX-2 metabolite-induced apoptosis to determine the role of iNOS. The results presented in Figs. 7(A and B) and 8(A and B), clearly show that L-NMMA can neither rescue cells from cell death nor inhibit caspase-3 activation ruling out the possibility of iNOS activation. These data further substantiate NADPH oxidase role in 15-LOX-2 metabolite-induced ROS generation and apoptosis.

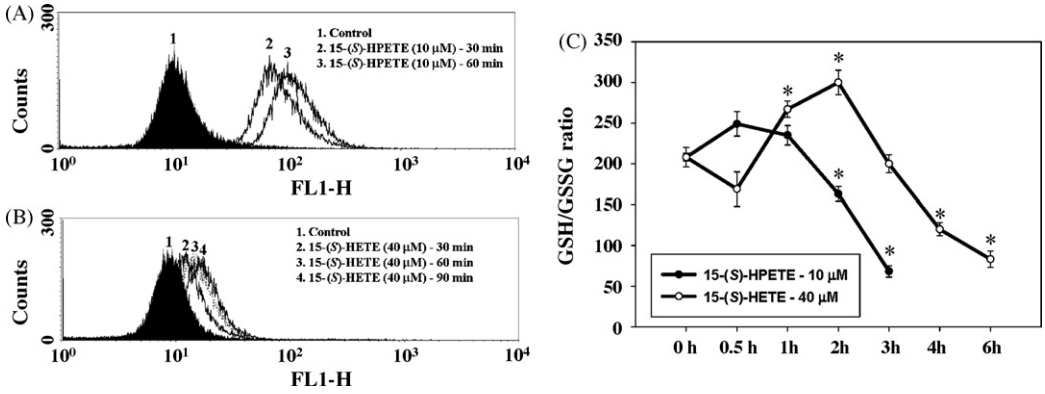

Fig. 5 – (A and B) 15-(S)-HPETE and 15-(S)-HETE induced ROS generation in K-562 cells. K-562 cells were incubated with 10 μM DCFH-DA for 15 min and then washed and incubated in PBS (containing 10 mM glucose) with either 10 μM 15-(S)-HPETE or 40 μM 15-(S)-HETE for indicated time periods. DCF fluorescence was detected by flow cytometry after stipulated treatments using 530 nm emission filter. (A) 1, control; 2, 10 μM 15-(S)-HPETE—30 min; 3, 10 μM 15-(S)-HPETE—60 min. (B) 1, control; 2, 40 μM 15-(S)-HETE—30 min; 3, 40 μM 15-(S)-HETE—60 min; 4, 40 μM 15-(S)-HETE—90 min. (C) Effect of 15-LOX-2 metabolites on glutathione depletion, as represented by GSH/GSSG ratio. GSH and GSSG levels were measured after treating K-562 cells with 15-(S)-HPETE (10 μM) and 15-(S)-HETE (40 μM) for indicated time periods. The cell lysates were treated with 10% sulfosalicylic acid (w/v) and the protein free extracts were used to measure GSH and GSSG levels by DTNB recycling assay. Data presented represent the mean ± S.E. of three independent experiments. The significance was established at $^{*}p < 0.05$ compared to 0 h treatments.

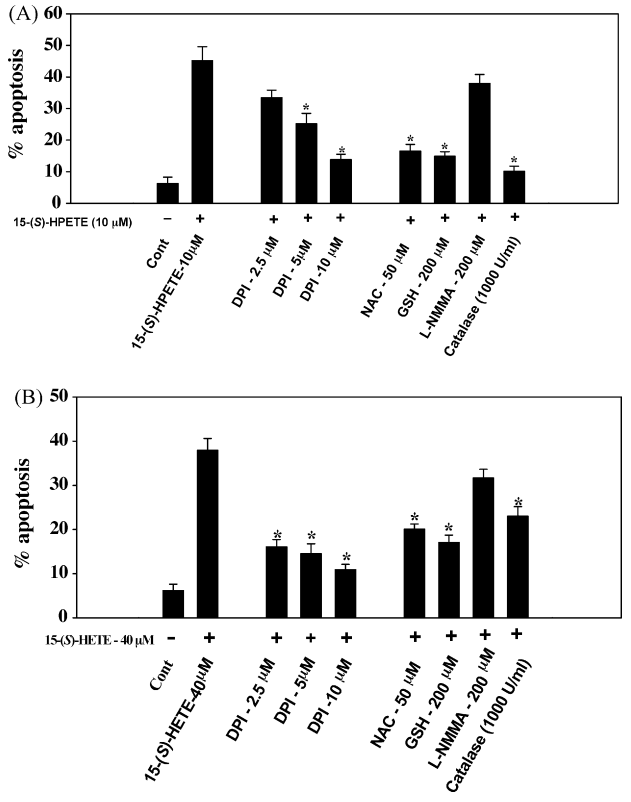

Fig. 7 – Inhibitory effects of NADPH oxidase inhibitor (DPI), iNOS inhibitor (L-NMMA), ROS inhibitors (NAC, GSH and catalase) on 15-LOX-2 metabolite-induced apoptosis. K-562 cells were pretreated with various classes of inhibitors—10 μM DPI (1 h)/200 μM L-NMMA (3 h)/50 μM NAC (3 h)/200 μM GSH (3 h)/1000 U/ml catalase (1 h) and followed by 15-LOX-2 metabolite treatment. (A) K-562 cells treated with various inhibitors and/or with 10 μM 15-(S)-HPETE as shown in the figure; (B) K-562 cells treated with various inhibitors and/or with 40 μM 15-(S)-HETE. Data represent mean ± S.E. from three independent experiments and the significance was established at $^{*}p < 0.05$ compared with respective 15-LOX-2 metabolite treatment.

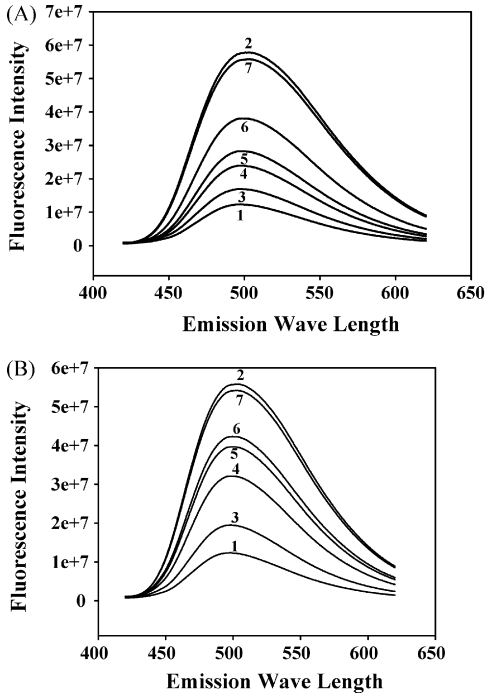

Fig. 8 – Inhibitory effects of 10 μM DPI (1 h)/50 μM NAC (3 h)/200 μM GSH (3 h)/200 μM L-NMMA (3 h)/1000 U/ml catalase (1 h) on 15-LOX-2 metabolite-induced caspase-3 activity. K-562 cells were pretreated with various classes of inhibitors followed by 15-LOX-2 metabolites as shown in the figure. (A) K-562 cells treated with various inhibitors and/or 15-(S)-HPETE (10 μM) (1, control; 2, 15-(S)-HPETE—10 μM (15HPT10); 3, catalase—1000 U/ml + 15HPT10; 4, NAC—50 μM + 15HPT10; 5, GSH—200 μM + 15HPT10; 6, DPI—10 μM + 15HPT10; 7, L-NMMA-200 μM + 15HPT10). (B) K-562 cells treated with various inhibitors and/or 15-(S)-HETE (40 μM) (1, control; 2, 15-(S)-HETE—40 μM (15HT40); 3, DPI—10 μM + 15HT40; 4, catalase—1000 U/ml + 15HT40; 5, NAC—50 μM + 15HT40; 6, GSH—200 μM + 15HT40; 7, L-NMMA-200 μM + 15HT40). Data represent one of the three independent experiments carried out.

3.7. *Effect of catalase on 15-LOX-2 metabolite-induced apoptosis*

Pretreatment with 1000 U/ml of catalase, an anti-oxidant enzyme, resulted in the inhibition of 15-(S)-HPETE induced apoptosis by 80% (Fig. 7A) and 15-(S)-HETE induced apoptosis by 55% (Fig. 7B). Pretreatment by Catalase also inhibited caspase-3 activation by 72% in 15-(S)-HPETE and by 42% in 15-(S)-HETE treatment (Fig. 8A and B).

3.8. *Cellular glutathione peroxidase levels and induction of apoptosis by 15-LOX-2 metabolites*

In view of differential effects of hydroperoxy and hydroxy metabolites, further studies were undertaken on the enzyme activity levels of GPx in K-562 and other leukemic cell lines, U-937, HL-60 and Jurkat for comparison. These studies revealed very low levels of GPx activity in K-562, Jurkat and high levels in U-937 cells (Fig. 10A). In the light of above, Jurkat (with low GPx) and U-937 (with high GPx) were treated with different concentrations of 15-(S)-HPETE and 15-(S)-HETE and analyzed by MTT assay. These studies illustrate that U-937 cell line, with high levels of GPx, was found to be highly resistant compared to Jurkat with low levels of GPx to 15-LOX-2 metabolite treatment (Fig. 10B).

4. Discussion

LOXs have been implicated in the pathogenesis of several disorders including asthma, allergy, inflammation, psoriasis and atherosclerosis. The relationship between LOXs and carcinogenesis is well established and recent studies show that various LOX pathways exist in a dynamic balance that shifts towards 5-, 8- and 12-LOXs and away from 15-LOX during carcinogenesis [7]. Even though the role of 15-LOX in

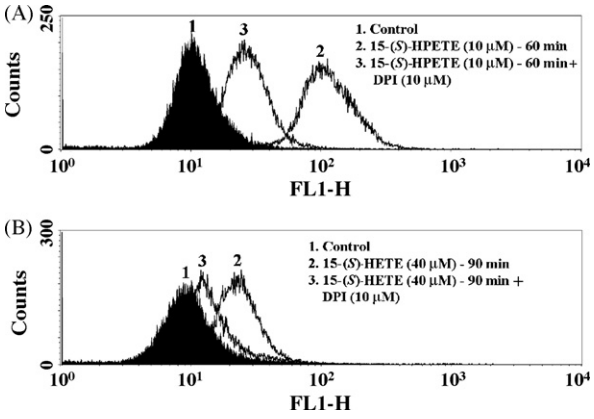

Fig. 9 – ROS analysis by DCFH-DA of K-562 cells pretreated with 10 μM DPI, an NADPH oxidase inhibitor for 1 h and followed by the treatment with 15-LOX-2 metabolites. (A) control; 2, 10 μM 15-(S)-HPETE—60 min; 3, 10 μM 15-(S)-HPETE—60 min + 10 μM DPI. (B) 1, control; 2, 40 μM 15-(S)-HETE—90 min; 3, 40 μM 15-(S)-HETE—90 min + 10 μM DPI. Data presented represent one of the three independent experiments.

mediating anti-carcinogenic effects was established, the mechanisms mediating these effects are still unclear. In this study, we analyzed the growth inhibitory effects of metabolites of 15-LOX-1 [13-(S)-HPODE and 13-(S)-HODE] and 15-LOX-2 [15-(S)-HPETE and 15-(S)-HETE] on chronic myeloid leukemia (K-562) cells. Both 15-(S)-HPETE and 15-(S)-HETE showed rapid growth inhibitory effects on K-562 cells, the former being more potent than the latter. Among 15-LOX-1 metabolites, 13-(S)-HPODE showed potent growth inhibitory effects but the hydroxy metabolite, 13-(S)-HODE, showed no significant effect even at concentrations as high as 80 μM. These results are in agreement with earlier reports where in 50 μM of 13-(S)-HODE did not inhibit the proliferation of colorectal carcinoma cells (Caco-2 and DLD-1) [26] and prostatic cancer cell lines (LNCaP, PC3 and DU145) [27]. Both phase-contrast and DAPI-DNA binding fluorescent microscopic studies showed that 15-(S)-HPETE and 15-(S)-HETE trigger cell death through induction of apoptosis in K-562 cells. K-562 cells treated with 10 μM 15-(S)-HPETE and 40 μM 15-(S)-HETE, revealed membrane blebbing, chromatin condensation, and formation of apoptotic bodies, all characteristic features of cells undergoing apoptosis. Flow cytometric analysis showed a prominent sub G0/G1 peak with both 15-(S)-HPETE and 15-(S)-HETE treatments. 15-(S)-HPETE treatment as shown in Fig. 2C resulted in 50% of cell death by 3 h where as 15-(S)-HETE showed similar effects at 40 μM concentration by 6 h. Similar effects have been observed with parent polyunsaturated fatty acids but only at very high concentrations [28]. DNA laddering, observed in 15-(S)-HPETE and 15-(S)-HETE treated cells further substantiates the induction of apoptosis by 15-LOX-2 metabolites.

Mitochondria play a key role in the activation of the caspase cascade via the release of cytochrome *c* from the mitochondrial intermembrane space [29]. Release of cytochrome *c* into the cytosol is one of the early events that initiate apoptosis. Consistent with these findings, we observed release of cytochrome *c* at earlier time points of exposure to 15-(S)-HPETE and 15-(S)-HETE. Once released into the cytosol, in the presence of dATP, cytochrome *c* participates in a protein-protein interaction with Apaf-1, which leads to the sequential activation of procaspase-9 and procaspase-3 [30]. In the present study the release of cytochrome c is followed by a clear time dependent activation of caspase-3. PARP cleavage products observed in K-562 cells exposed to 15-(S)-HPETE and 15-(S)-HETE provides an evidence for the caspase-3 activation during 15-LOX-2 metabolite-induced apoptosis. These findings demonstrate that 15-LOX-2 metabolites induce apoptosis by activating the intrinsic death pathway through a series of events involving cytochrome *c* release, caspase-3 activation, PARP cleavage and DNA fragmentation.

Cytochrome *c* leakage is associated with mitochondrial permeability transition perturbations and generation of reactive oxygen species (ROS) [31–33]. The possible involvement

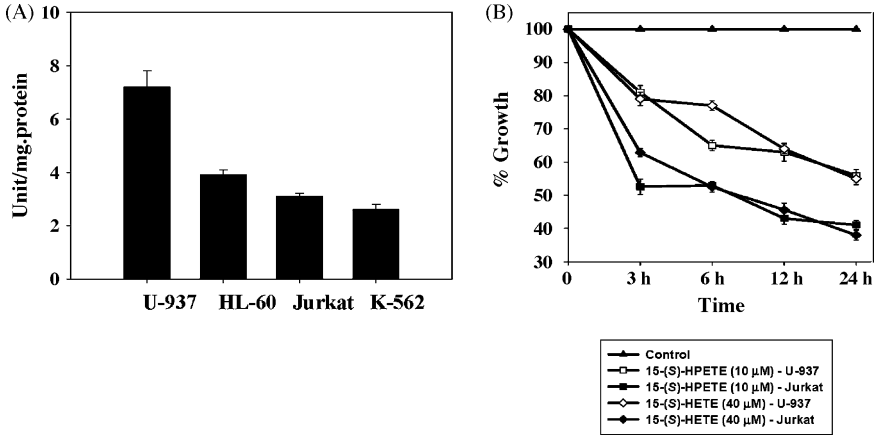

Fig. 10 – (A) Analysis of glutathione peroxidase levels in various cancer cell lines as indicated and the activity is represented as units/mg protein. One unit of GPx activity was defined as one nmole of NADPH oxidized per min. The values represent the mean ± S.E. from three independent experiments; (B) growth inhibitory effects of 15-LOX-2 metabolites on U-937 and Jurkat cell lines. 5×10^3 cells were treated with 10 μM 15-(S)-HPETE and 40 μM 15-(S)-HETE for 3, 6, 12 and 24 h and analyzed by MTT assay as described in methodology. Data presented represent the mean ± S.E. from three independent experiments.

of ROS generation in 15-LOX-2 metabolite-induced apoptosis investigated through DCFH-DA analysis in the present study indicates that there is many-fold induction of ROS within minutes of 15-LOX-2 metabolite treatment. This is associated with the depletion of cellular glutathione levels, the cellular anti-oxidant defense system, which paralleled the apoptotic induction; *N*-acetyl cysteine (NAC), a glutathione precursor and reduced glutathione (GSH) have diminished the ROS production induced by 15-LOX-2 metabolites and inhibited subsequent activation of caspase-3 and induction of apoptosis. DPI, an NADPH oxidase inhibitor has reduced ROS produced by both 15-(*S*)-HPETE and 15-(*S*)-HETE, abrogated the activation of caspase-3 and subsequent induction of apoptosis. These results clearly indicate that ROS generated through the activation of NADPH oxidase is an upstream event of cytochrome *c* release and caspase activation in 15-LOX-2 metabolite-induced apoptosis. Several independent studies have shown that NADPH oxidase-mediated ROS generation is critical to trigger apoptosis [34]. DPI also inhibits other flavoprotein-using enzymes, such as inducible nitric oxide synthase (iNOS) [25]. However, L-NMMA, a more specific inhibitor of iNOS did not inhibit 15-LOX-2 metabolite-induced apoptosis significantly, demonstrating that nitric oxide and reactive nitrogen intermediates are not involved in 15-LOX-2 metabolite-induced apoptosis. These observations reinforce our hypothesis that NADPH oxidase generated ROS mediates 15-LOX-2 metabolite-induced apoptosis.

Pretreatment of cells with catalase inhibited the apoptosis induced by 15-(*S*)-HPETE to a larger extent and partially inhibited apoptosis induced by 15-(*S*)-HETE. Inhibiton of apoptosis by catalase pretreatment suggests that H_2O_2 is being accumulated within the cells upon 15-LOX-2 metabolite treatment. ROS generation shown earlier by DCFH-DA analysis further supports such a possibility. Glutathione peroxidase (GPx) across the cell lines is the principal enzyme in reducing hydroperoxy metabolites to less toxic hydroxy metabolites [35]. The levels of GPx are varying across the cell lines (K-562, Jurkat, HL-60 and U-937) and there is a direct relevance to the anti-proliferative effects of 15-LOX-2 metabolites and GPx levels in the cell line. Both, 15-(*S*)-HPETE, the hydroperoxy metabolite and 15-(*S*)-HETE, hydroxy metabolite, showed diminished anti-proliferative effects in cells with high peroxidase activity. 15-(*S*)-HETE, though required in higher concentrations, induced apoptosis through a mechanism similar to that of 15-(S)-HPETE. In contrast to the hydroxy metabolite of 15-LOX-2 [15-(*S*)-HETE], the hydroxy metabolite of 15-LOX-1 [13-(*S*)-HODE] did not induce apoptosis until very high concentrations were applied. In the light of these differential anti-proliferative effects of 15-LOX metabolites on the cell lines with varied levels of GPx, we hypothesize that 15-(*S*)-HETE undergoes further oxygenations inside the K-562 cells and these oxygenated metabolites induce apoptosis. Our hypothesis draws support from earlier observations that 15-(*S*)-HETE which has got additional doubly allelic methylene groups can undergo further oxygenation once entered into the cell [36]. 13-(*S*)-HODE, however, lacks these groups to undergo further oxygenation. 15-(*S*)-HETE, after entering the cell can be converted to a hydroperoxy, hydroxy metabolite like 5-hydroperoxy-15-(*S*)-HETE or 8-hydroperoxy-15-(*S*)-HETE depending on the type of LOX present in the cell, which subsequently generates ROS and induces apoptosis. In support of this hypothesis, chronic myeloid leukemia cells have been shown to contain other LOX enzymes [37,38].

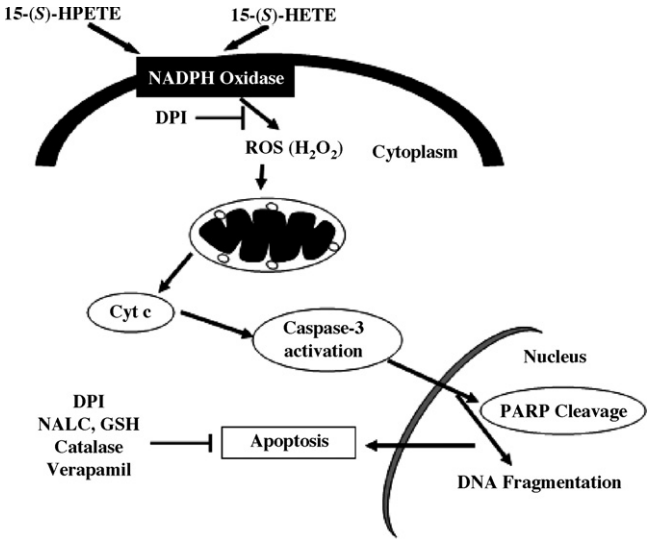

Fig. 11 – Scheme depicting the proposed mechanism of induction of apoptosis in K-562 cells by 15-(*S*)-HPETE and 15-(*S*)-HETE.

In the current study, we have shown the differential ability of 15-LOX metabolites to exert growth inhibitory effects and rapid induction of apoptosis in chronic myeloid leukemia (K-562) cell line. We have further delineated the pathway of apoptotic induction by 15-LOX-2 metabolites and the molecular mechanisms associated with it. Our results clearly indicate that the apoptosis induced by 15-(*S*)-HPETE and 15-(*S*)-HETE is associated with the release of cytochrome *c*, activation of caspase-3, PARP cleavage and DNA fragmentation. We have shown for the first time that ROS produced by NADPH oxidase activation is responsible for the 15-LOX-2 metabolite-induced apoptosis through intrinsic death pathway (Fig. 11). In the present study, we come up with a hypothesis that addresses the discrepancies existing between the differential effects shown by the two 15-LOX isoforms and their hydroperoxy and hydroxy metabolites.

Acknowledgements

This work was supported by research grants from: (a) Department of Science and Technology, New Delhi and Dabur Research Foundation, Ghaziabad, India (Grant #VI-D and P/11/2001-TT) and (b) Institute of Life Sciences, Hyderabad (Grant #EFL/II/CS-MoU/112/1869). We duly acknowledge Council of Scientific and Industrial Research (CSIR), Govt. of India for providing Research Fellowship to S.V.K. Mahipal, J. Subhashini, M. Mallikarjun Reddy and Karnati R. Roy.

REFERENCES

[1] Yamamoto S. Mammalian lipoxygenases: molecular structures and functions. Biochim Biophys Acta 1992;1128:117–31.

[2] Meruvu S, Walther M, Ivanov I, Hammarstrom S, Furstenberger G, Krieg P, et al. Sequence determinants for the reaction specificity of murine (12R)-lipoxygenase: targeted substrate modification and site-directed mutagenesis. J Biol Chem 2005;280:36633–41.
[3] Shureiqi I, Lippman SM. Lipoxygenase modulation to reverse carcinogenesis. Cancer Res 2001;61:6307–12.
[4] Bhatia B, Maldonado C, Tang SH, Chandra D, Klein RD, Chopra D, et al. Sub-cellular localization and tumor suppressive functions of 15-lipoxygenase 2 (15-LOX2) and its splice variants. J Biol Chem 2003;278: 25091–100.
[5] Ikawa H, Kamitani H, Calvo BF, Foley JF, Eling TE. Expression of 15-lipoxygenase-1 in human colorectal cancer. Cancer Res 1999;59:360–6.
[6] Kelavkar UP, Cohen C, Kamitani H, Eling TE, Badr KF. Concordant induction of 15-lipoxygenase-1 and mutant p53 expression in human prostate adenocarcinoma: correlation with Gleason staging. Carcinogenesis 2000;21:1777–87.
[7] Shureiqi I, Wojno KJ, Poore JA, Reddy RG, Moussalli MJ, Spindler SA, et al. Decreased 13-S- hydroxyoctadecadienoic acid levels and 15-lipoxygenase-1 expression in human colon cancers. Carcinogenesis 1999;20:1985–95.
[8] Hsi LC, Xi X, Lotan R, Shureiqi I, Lippman SM. The histone deacetylase inhibitor suberoylanilide hydroxamic acid induces apoptosis via induction of 15-lipoxygenase-1 in colorectal cancer cells. Cancer Res 2004;64: 8778–81.
[9] Kamitani H, Taniura S, Ikawa H, Watanabe T, Kelavkar UP, Eling TE. Expression of 15-lipoxygenase-1 is regulated by histone acetylation in human colorectal carcinoma. Carcinogenesis 2001;22:187–91.
[10] Shureiqi I, Chen D, Lee JJ, Yang P, Newman RA, Brenner DE, et al. 15-LOX-1: a novel molecular target of nonsteroidal anti-inflammatory drug-induced apoptosis in colorectal cancer cells. J Natl Cancer Inst 2000;92:1136–42.
[11] Shappell SB, Gupta RA, Manning S, Whitehead R, Boeglin WE, Schneider C, et al. 15S-Hydroxyeicosatetraenoic acid activates peroxisome proliferator-activated receptor gamma and inhibits proliferation in PC3 prostate carcinoma cells. Cancer Res 2001;61:497–503.
[12] Kiran Kumar YV, Raghunathan A, Sailesh S, Prasad M, Vemuri MC, Reddanna P. Differential effects of 15-HPETE and 15-HETE on BHK-21 cell proliferation and macromolecular composition. Biochim Biophys Acta 1993;1167:102–8.
[13] Maccarrone M, Ranalli M, Bellincampi L, Salucci ML, Sabatini S, Melino G, et al. Activation of different lipoxygenase isozymes induces apoptosis in human erythroleukemia and neuroblastoma cells. Biochem Biophys Res Commun 2000;272:345–50.
[14] Reddy GR, Reddanna P, Reddy CC, Curtis WR. 11-Hydroperoxyeicosatetraenoic acid is the major dioxygenation product of lipoxygenase isolated from hairy root cultures of Solanum tuberosum. Biochem Biophys Res Commun 1992;189:1349–52.
[15] Sailesh S, Kumar YV, Prasad M, Reddanna P. Sheep uterus dual lipoxygenase in the synthesis of 14,15-leukotrienes. Arch Biochem Biophys 1994;315:362–8.
[16] Mosmann T. Rapid colorimetric assay for cellular growth and survival: application to proliferation and cytotoxicity assays. J Immunol Methods 1983;65:55–63.
[17] Herrmann M, Lorenz HM, Voll R, Grunke M, Woith W, Kalden JR. A rapid and simple method for the isolation of apoptotic DNA fragments. Nucleic Acids Res 1994;22: 5506–7.
[18] Reddy MC, Subhashini J, Mahipal SV, Bhat VB, Srinivas Reddy P, Kiranmai G, et al. C-Phycocyanin, a selective cyclooxygenase-2 inhibitor, induces apoptosis in lipopolysaccharide-stimulated RAW 264.7 macrophages. Biochem Biophys Res Commun 2003;304:385–92.
[19] Sambrook J, Frotsch CF, Maniatis T. Molecular cloning. Plain view. Coldspring Harbour; 1999.
[20] Bradford MM. A rapid and sensitive method for the quantitation of microgram quantities of protein utilizing the principle of protein-dye binding. Anal Biochem 1976;72:248–54.
[21] Bass DA, Parce JW, Dechatelet LR, Szejda P, Seeds MC, Thomas M. Flow cytometric studies of oxidative product formation by neutrophils: a graded response to membrane stimulation. J Immunol 1983;130:1910–7.
[22] Cathcart R, Schwiers E, Ames BN. Detection of picomole levels of hydroperoxides using a fluorescent dichlorofluorescein assay. Anal Biochem 1983;134: 111–6.
[23] Tietze F. Enzymic method for quantitative determination of nanogram amounts of total and oxidized glutathione: applications to mammalian blood and other tissues. Anal Biochem 1969;27:502–22.
[24] Paglia DE, Valentine WN. Studies on the quantitative and qualitative characterization of erythrocyte glutathione peroxidase. J Lab Clin Med 1967;70:158–69.
[25] Stuehr DJ, Fasehun OA, Kwon NS, Gross SS, Gonzalez JA, Levi R, et al. Inhibition of macrophage and endothelial cell nitric oxide synthase by diphenyleneiodonium and its analogs. FASEB J 1991;5:98–103.
[26] Nixon JB, Kim KS, Lamb PW, Bottone FG, Eling TE. 15-Lipoxygenase-1 has anti-tumorigenic effects in colorectal cancer. Prostaglandins Leukot Essent Fatty Acids 2004;70: 7–15.
[27] Tang S, Bhatia B, Maldonado CJ, Yang P, Newman RA, Liu J, et al. Evidence that arachidonate 15-lipoxygenase 2 is a negative cell cycle regulator in normal prostate epithelial cells. J Biol Chem 2002;277:16189–201.
[28] Jiang WG, Bryce RP, Horrobin DF. Essential fatty acids: molecular and cellular basis of their anti-cancer action and clinical implications. Crit Rev Oncol Hematol 1998;27: 179–209.
[29] Liu X, Kim CN, Yang J, Jemmerson R, Wang X. Induction of apoptotic program in cell-free extracts: requirement for dATP and cytochrome c. Cell 1996;86:147–57.
[30] Li P, Nijhawan D, Budihardjo I, Srinivasula SM, Ahmad M, Alnemri ES, et al. Cytochrome c and dATP-dependent formation of Apaf-1/caspase-9 complex initiates an apoptotic protease cascade. Cell 1997;91:479–89.
[31] Chandra J, Samali A, Orrenius S. Triggering and modulation of apoptosis by oxidative stress. Free Radic Biol Med 2000;29:323–33.
[32] Martindale JL, Holbrook NJ. Cellular response to oxidative stress: signaling for suicide and survival. J Cell Physiol 2002;192:1–15.
[33] Tan S, Sagara Y, Liu Y, Maher P, Schubert D. The regulation of reactive oxygen species production during programmed cell death. J Cell Biol 1998;141:1423–32.
[34] Coxon A, Rieu P, Barkalow FJ, Askari S, Sharpe AH, von Andrian UH, et al. A novel role for the beta 2 integrin CD11b/CD18 in neutrophil apoptosis: a homeostatic mechanism in inflammation. Immunity 1996;5:653–66.
[35] Kuhn H, Walther M, Kuban RJ. Mammalian arachidonate 15-lipoxygenases structure, function, and biological implications. Prostaglandins Other Lipid Mediat 2002; 68–69:263–90.
[36] Chavis C, Vachier I, Chanez P, Bousquet J, Godard P. 5(S), 15(S)-dihydroxy-eicosatetraenoic acid and lipoxin generation in human polymorphonuclear cells: dual

specificity of 5-lipoxygenase towards endogenous and exogenous precursors. J Exp Med 1996;183:1633–43.
[37] Maccarrone M, Putti S, Finazzi Agro A. Altered gravity modulates 5-lipoxygenase in human erythroleukemia K562 cells. J Gravit Physiol 1998;5:97–8.
[38] Maccarrone M, Lorenzon T, Guerrieri P, Agro AF. Resveratrol prevents apoptosis in K562 cells by inhibiting lipoxygenase and cyclooxygenase activity. Eur J Biochem 1999;265: 27–34.